Light scattering characterization of mitochondrial aggregation in single cells

Xuan-Tao Su[a], Kirat Singh[a], Wojciech Rozmus[a], Christopher Backhouse[b], and Clarence Capjack[b]

[a]*Department of Physics, University of Alberta, Edmonton, T6G 2G7, Canada*
[b]*Department of Electrical & Computer Engineering, University of Alberta, Edmonton, T6G 2V4, Canada*
xtsu@phys.ualberta.ca

Abstract: Three dimensional finite-difference time-domain (FDTD) simulations are employed to show that light scattering techniques may be used to infer the mitochondrial distributions that exist within single biological cells. Two-parameter light scattering plots of the FDTD light scattering spectra show that the small angle forward scatter can be used to differentiate the case of a random distribution of mitochondria within a cell model from that in which the mitochondria are aggregated to the nuclear periphery. Fourier transforms of the wide angle side scatter spectra show a consistent highest dominant frequency, which may be used for size differentiation of biological cells with distributed mitochondria.

OCIS codes: (170.1530) Cell analysis; (170.1610) Clinical applications; (290.0290) Scattering; (000.1430) Mitochondria; (000.4430) Finite-Difference Time-Domain

References and links

1. A. Dunn, and R. Richards-Kortum, "Three-dimensional computation of light scattering from cells," IEEE J. Sel. Top. Quantum Electron. **2**(4), 898–905 (1996).
2. C. G. Liu, C. Capjack, and W. Rozmus, "3-D simulation of light scattering from biological cells and cell differentiation," J. Biomed. Opt. **10**(1), 014007 (2005).
3. J. Q. Lu, P. Yang, and X. H. Hu, "Simulations of light scattering from a biconcave red blood cell using the finite-difference time-domain method," J. Biomed. Opt. **10**(2), 024022 (2005).
4. J. R. Mourant, J. P. Freyer, A. H. Hielscher, A. A. Eick, D. Shen, and T. M. Johnson, "Mechanisms of light scattering from biological cells relevant to noninvasive optical-tissue diagnostics," Appl. Opt. **37**(16), 3586–3593 (1998).
5. X. Li, A. Taflove, and V. Backman, "Recent progress in exact and reduced-order modeling of light-scattering properties of complex structures," IEEE J. Sel. Top. Quantum Electron. **11**(4), 759–765 (2005).
6. K. S. Yee, "Numerical Solution of Initial Boundary Value Problems Involving Maxwells Equations in Isotropic Media," IEEE Trans. Antenn. Propag. **AP14**, 302–307 (1966).
7. A. Taflove, and S. C. Hagness, *Computational Electrodynamics: The Finite-Difference Time-Domain Method*, (Artech House, Norwood, MA, 2005).
8. X. T. Su, C. Capjack, W. Rozmus, and C. Backhouse, "2D light scattering patterns of mitochondria in single cells," Opt. Express **15**(17), 10562–10575 (2007).
9. P. L. Gourley, J. K. Hendricks, A. E. McDonald, R. G. Copeland, K. E. Barrett, C. R. Gourley, and R. K. Naviaux, "Ultrafast nanolaser flow device for detecting cancer in single cells," Biomed. Microdevices **7**(4), 331–339 (2005).
10. W. D. Thomas, X. D. Zhang, A. V. Franco, T. Nguyen, and P. Hersey, "TNF-related apoptosis-inducing ligand-induced apoptosis of melanoma is associated with changes in mitochondrial membrane potential and perinuclear clustering of mitochondria," J. Immunol. **165**(10), 5612–5620 (2000).
11. L. Y. Liu, A. Vo, G. Q. Liu, and W. L. McKeehan, "Distinct structural domains within C19ORF5 support association with stabilized microtubules and mitochondrial aggregation and genome destruction," Cancer Res. **65**(10), 4191–4201 (2005).
12. E. Alirol, and J. C. Martinou, "Mitochondria and cancer: is there a morphological connection?" Oncogene **25**(34), 4706–4716 (2006).
13. R. H. Carlson, C. V. Gabel, S. S. Chan, R. H. Austin, J. P. Brody, and J. W. Winkelman, "Self-sorting of white blood cells in a lattice," Phys. Rev. Lett. **79**(11), 2149–2152 (1997).
14. Z. P. Liao, H. L. Wong, B. Yang, and Y. Yuan, "A Transmitting Boundary for Transient Wave Analyses," Scientia Sinica Series **27**, 1063–1076 (1984).
15. G. Mur, "Absorbing Boundary-Conditions for the Finite-Difference Approximation of the Time-Domain Electromagnetic-Field Equations," IEEE Trans. Electromagn. Compat. **23**(4), 377–382 (1981).

#104397 - $15.00 USD Received 21 Nov 2008; revised 1 Jun 2009; accepted 15 Jul 2009; published 20 Jul 2009

16. J. P. Berenger, "A Perfectly Matched Layer for the Absorption of Electromagnetic-Waves," J. Comput. Phys. **114**(2), 185–200 (1994).
17. H. M. Shapiro, *Practical Flow Cytometry*, (John Wiley & Sons, Inc., Hoboken, NJ, 2003).
18. M. Kerker, H. Chew, P. J. McNulty, J. P. Kratohvil, D. D. Cooke, M. Sculley, and M. P. Lee, "Light scattering and fluorescence by small particles having internal structure," J. Histochem. Cytochem. **27**(1), 250–263 (1979).
19. X. T. Su, K. Singh, C. Capjack, J. Petrácek, C. Backhouse, and W. Rozmus, "Measurements of light scattering in an integrated microfluidic waveguide cytometer," J. Biomed. Opt. **13**(2), 024024 (2008).
20. Z. Wang, J. El-Ali, M. Engelund, T. Gotsaed, I. R. Perch-Nielsen, K. B. Mogensen, D. Snakenborg, J. P. Kutter, and A. Wolff, "Measurements of scattered light on a microchip flow cytometer with integrated polymer based optical elements," Lab Chip **4**(4), 372–377 (2004).

1. Introduction

Light scattering techniques have been reported to provide a label-free characterization of biological cells or tissues [1–5]. Mourant *et al*. suggested that organelles with sizes similar to that of mitochondria are the dominant scatterers for the light scattering measured from intact biological cells [4]. The contributions of organelles (for example, mitochondria) to light scattering from biological cells have also been studied by the finite-difference time-domain (FDTD) simulations [1,2], where the FDTD method is based on Yee algorithm [6] and can be used to numerically solve Maxwell's equations [7]. Recently, Su *et al*. reported that mitochondria dominate the 2D light scatter patterns from human Raji cells [8], and the experimental results were compared with FDTD simulations. A better understanding of light scattering from mitochondria in human cells requires further quantitative measurements and/or simulations. For example, the population of mitochondria in biological cells can have different distributions which in turn may affect the observed light scattering. It has been recently observed that mitochondrial aggregation to the nuclear periphery will occur in normal cells, while mitochondria are randomly distributed in cancerous cells [9]. Peri-nuclear clustering of mitochondria has also been observed in anti-cancer agent treated malignant cells, while mitochondria are widely distributed in the untreated malignant cells [10,11]. Fluorophore-labeling techniques have been used to observe these mitochondrial distributions in cells [9–11]. A label free, non-invasive light scattering method that could detect mitochondrial aggregation in single cells would be useful in clinical cancerous cell detection.

In this paper, we explore the use of a light scattering approach for inferring mitochondrial distributions in single biological cells. In particular, we compare scattering from a cell model in which mitochondria are randomly distributed with that in which the mitochondria are aggregated to the nuclear periphery. Simulations of light scattering from these two types of cell models are performed by using a 3D FDTD algorithm. A two-parameter light scattering plot method is proposed for differentiating these two cases based on the analyses of the FDTD light scattering spectra. Although real biological cells are more complex than the models considered here because of the presence of mitochondria of varying sizes and non-spherical structures, and the presence of fusion and interconnected networks [9,12], this is a first step towards understanding the effects of mitochondrial distributions on the light scattering from human cells.

2. Simulation methods

A Monte Carlo computer code was written to generate three different mitochondrial distributions in single cell models. In one case, the mitochondria are aggregated to the nuclear periphery and will be referred to as the "normal cell" model. For the second case, the mitochondria are randomly distributed within the cell and will be referred to as the "cancer cell" model. For the third case, the mitochondria are aggregated to the cell membrane and this case represents an extreme state of a "cancer cell" model. The motivation for referring to the three different mitochondrial distribution models as normal or cancerous cells is that the corresponding distributions are typically found in actual biological cells [9–11]. The geometry for these models is shown in Fig. 1(a). Both the cell and the nucleus are assumed to be centered at the origin. Zones I, II, and III in Fig. 1(a) are used to differentiate the different mitochondrial distributions by counting the mitochondria numbers centered in each of these zones. For example, the number of mitochondria in zone I should be larger for mitochondrial

#104397 - $15.00 USD Received 21 Nov 2008; revised 1 Jun 2009; accepted 15 Jul 2009; published 20 Jul 2009

aggregation to the nucleus periphery as compared with the randomly distributed mitochondria in a cell model. To generate the different cell models, the probability ρ of finding a mitochondrion at a distance R_d (center of a mitochondrion to the center of the nucleus) in a cell is given as (all sizes in μm):

$$\rho = \rho_0 \exp(-(R_d - r_n - r_m - \delta_m)/\alpha) \tag{1}$$

$$\rho = 0.5 \tag{2}$$

$$\rho = \rho_0 \exp(-(r_c - R_d - r_m - \delta_m)/\alpha) \tag{3}$$

Here r_n is the radius of the nucleus, r_m is the radius of the mitochondrion, r_c is the radius of the cell, and δ_m is the smallest distance between any two organelles, ρ_0 and α are constants for the probability distribution. In this paper the thicknesses of zone I and zone III are defined as $r_m + \delta_d$, where δ_d is a constant smaller than $(r_c - r_n - 2r_m)/2$. In this case, the thickness of zone II is given by $(r_c - r_n - 2(r_m + \delta_d))$. The Eq. (1) above describes mitochondrial aggregation to the nuclear periphery, Eq. (2) describes randomly distributed mitochondria within the cell and Eq. (3) describes mitochondrial aggregation to the cell membrane.

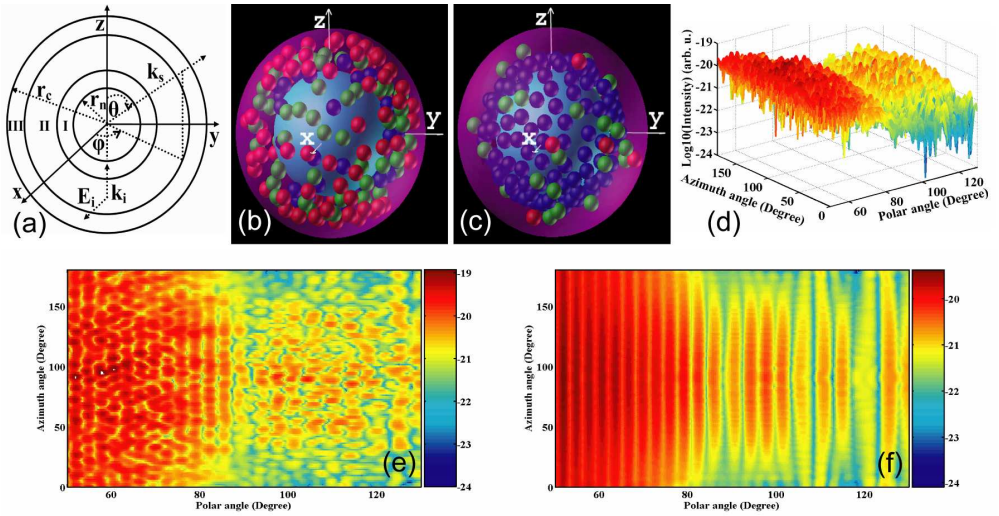

Fig. 1. 3D biological cell models and FDTD scatter spectra. (a), Geometry for the study of mitochondrial distributions in single cells. (b), randomly distributed mitochondria in a single cell. (c), mitochondrial aggregation to the nuclear periphery in a single cell. Blue spheres denote the mitochondria centered in zone I, green in zone II, and red in zone III. The cell has a nucleus (cyan color) centered at the origin. The cell cytoplasm is shown in magenta. (d) and (e) are FDTD 3D light scattering pattern and 2D light scattering pattern for cell model (b), respectively. (f) is an FDTD 2D light scattering pattern for a cell model without mitochondria.

In this paper, we use $\rho_0 = 0.6$, $\alpha = 0.1$ μm, $\delta_d = 0.3$ μm, $\delta_m = 0.01$ μm, $r_m = 0.4$ μm [1], $r_n = 3.0$ μm and $r_c = 5.0$ μm [13] for the modeling of the biological cells. The total mitochondria number is fixed as 180 in a single cell model, which occupies a volume fraction of 9.22% (180 mitochondria with radii of 0.4 μm) in a cell of 5.0μm in radius [1]. The constants here are chosen to give a reasonable mitochondrial distribution. For example, if α is set to 0.01μm instead of 0.1μm in Eq. (3), all the 180 mitochondria will be distributed in Zone III as tested for different random seeds. Eight different random seeds are assigned to generate eight realizations for each different mitochondrial distribution via a Monte Carlo method as determined by Eqs. (1) to (3). In this case, for each random seed the mitochondria can have three different distributions. For the same kind of mitochondrial distribution, the eight

#104397 - $15.00 USD Received 21 Nov 2008; revised 1 Jun 2009; accepted 15 Jul 2009; published 20 Jul 2009

different random seeds generate eight realizations but do not significantly change the mitochondria numbers in each of the zones I, II and III. Note that all the eight realizations for each different mitochondrial distribution were generated arbitrarily and we believe that they are representative for the differentiation of the different mitochondrial distributions. Visualizations of the representative 3D biological cell models are shown in Figs. 1(b) and (c), for a "cancer cell" and a "normal cell" model, respectively. There are 36 mitochondria in zone I, 67 in zone II, and 77 in zone III for the distribution given by "cancer cell" model Fig. 1(b). For the "normal cell" model as shown in Fig. 1(c), there are 142 mitochondria in zone I, 33 in zone II, and 5 in zone III.

Three dimensional FDTD simulations are used to study light scattering from these three mitochondrial distribution models. In this paper, a Liao boundary condition [14] is used to terminate the FDTD 3D grids, due to its improved performance over the Mur boundary condition [15], and the reduced computational storage memory requirements as compared with the perfectly matched layer (PML) boundary condition [16]. The numerical simulation results obtained with our FDTD algorithm have been shown agreed well with analytical Mie theory results [2]. The step size that is used here is approximately 40nm, with an incident wavelength of 632.8nm. The geometry for the FDTD code is shown in Fig. 1(a). The incident plane wave has a wave vector $\hat{k}_i$ along the $\hat{z}$ direction, and is polarized along the $\hat{x}$ direction. The scattered wave $\hat{k}_s$ has an azimuth angle φ, and a polar angle θ. The refractive index for the cell cytoplasm is 1.38, 1.39 for the nucleus, and 1.42 for the mitochondria [1,8]. The surrounding medium has a refractive index of 1.334. For the 3D FDTD simulation of each cell model in this paper, it requires approximately 24 running hours with parallel computations on 64 CPUs, each with a memory of 0.5GB.

3. Results and discussion

In order to study the mitochondrial aggregation effects in the single biological cell models, eight arbitrary different random seeds are used to generate twenty four realizations as described above (each kind of mitochondrial distribution has eight different realizations). The representative 3D scatter pattern and 2D scatter pattern for the cell model in Fig. 1(b) are shown in Fig. 1(d) and (e), respectively. The 2D scatter patterns are the contour plots of the 3D scatter patterns in a plane surface. Figure 1(f) is an FDTD 2D scatter pattern for a cell model without mitochondria (with only the cell cytoplasm and a nucleus as shown in Fig. 1(b)). These 2D scatter patterns are similar to those obtained by using a 2D cytometric technique (experimental patterns are compared with FDTD simulations), where the cell nucleus and the cell cytoplasm contribute to band structures and the mitochondria contribute to small scale 2D structures [8]. The 3D scatter patterns contain rich information about the biological cell models. As a first step, in this paper we perform an analysis of the scattered light for a given range of polar angle θ with the azimuth angle fixed at $\varphi = 90$ degrees, *i.e.*, a cross section scanning of the 2D light scattering patterns.

In Fig. 2, we show the light scattering spectra of different cell models in different angular ranges and the method to differentiate mitochondrial distributions in single cell models. In Fig. 2(a), the cases for different mitochondrial distributions are shown in the angular range 0~10 degrees. For each case of mitochondrial distribution in Fig. 2(a), there are eight different realizations. The inset in Fig. 2(a) shows a comparison of results for the following cases: (i) mitochondrial aggregation to the cell membrane, (ii) a mitochondrial random distribution and (iii) mitochondrial aggregation to the nucleus, over the entire scattering polar angle. Figure 2(b) and Fig. 2(c) each give the scattered intensities for eight different realizations of a random mitochondrial distribution. Figure 2(b) gives the scattered intensity in the small angle forward scattering range (0 to 1 degrees) while Fig. 2(c) gives the side scattered intensity (85 to 95 degrees). Intensity variations in Fig. 2(b) are far less than the minimum intensity variation between different cases of mitochondrial distributions such as those shown in Fig. 2(a). Figure 2(c) shows that the light scattering distributions in the side scatter angular range have a more complex structure as compared with the small angle forward scatter shown in

#104397 - $15.00 USD Received 21 Nov 2008; revised 1 Jun 2009; accepted 15 Jul 2009; published 20 Jul 2009

Figs. 2(a) and (b). Small angle forward scatter and side scatter are the two angular ranges that are of most interest in this paper. Integrations of the area under the light scattering intensity spectra as shown in Figs. 2(a), (b) and (c) in these angular ranges are performed in order to differentiate the three cases of mitochondrial distributions.

Two-parameter light scattering plots have been used in cytometry to give better understanding of the cellular measurements [17]. In Fig. 2(d), we construct two-parameter light scattering plots. The vertical axis shows the integration of the scattered light intensity for small angle forward scattering (0~5 degrees), while the horizontal axis shows the integrated intensity of light scattering around the 90 degree scatter (85~95 degrees). The open signs are for the twenty four realizations with a cell radius of 5.0μm, and the solid signs are another six realizations with a cell radius of 5.1μm. The three different mitochondrial distribution cases that are considered lead to different results along the horizontal axis as shown in Fig. 2(d). However the more distinctive differences between the three cases are along the vertical axis, which is in the small angle forward scattering. In order to quantify the difference in scattering between the different mitochondrial distribution models, the mean and standard deviation (SD) of the intensity of different cases are calculated, for the values along the vertical axis in Fig. 2(d). For the case of mitochondrial aggregation to the cell membrane, the mean is 0.7979 (arb. u.) with a SD of 0.0073 (arb. u.). The mean is 0.7234 (arb. u.) with a SD of 0.0073 (arb. u.) for the case of randomly distributed mitochondria, while the mean is 0.6326 (arb. u.) with a SD of 0.0031 (arb. u.) for the case of mitochondrial aggregation to the nucleus periphery. The differences between the means of the "normal cell" models and "cancer cell" models are 0.1653 (arb. u.) and 0.0908 (arb. u.), which are at least 10 times larger than any SD of the three different cases of mitochondrial distributions. As it is well known in conventional flow cytometry, the small angle forward scattering is assumed to be determined by the overall cell size [17,18]. Here we use the small angle forward scattering for the differentiation of mitochondrial distributions. Thus we would like to study the effects of cell size variations on the method of two-parameter light scattering plots. Two arbitrary realizations for each mitochondrial distribution with a cell model radius of 5.1μm are generated. This is, for a cell volume variation of 6.12% (that is, the 5.1μm cell model has a volume of approximately 106.12% that of the 5.0μm cell model). The nucleus size and position, the mitochondria size and total numbers are kept unchanged. We found that the mean for the case of mitochondria random distribution (eight realizations for the 5.0μm cell, and two realizations for the 5.1μm cell) is 0.7200 (arb. u.) as compared with 0.7234 (arb. u.) for the eight realizations for the cell size of 5.0μm in radius. Thus the case for the mitochondrial aggregation to the nuclear periphery can still be well differentiated from the case where the mitochondria are randomly distributed or aggregated to the membrane for a cell volume variation of 6.12% as shown in Fig. 2(d).

Above we have discussed the two-parameter light scattering plots for the differentiation of mitochondrial distributions in biological cell models with cell size variations. However other cell components variations, such as the mitochondria size and volume fraction variations, nucleus variations and biological cell shape variations may also change the small angle forward scattering. In order to study this we have generated another three realizations for mitochondrial random distributions. To study the effects of mitochondria variations on the two-parameter light scattering plots method, we assume that each of the 180 mitochondria has a radius of 420nm in a biological cell model of 5μm in radius. The nucleus radius is assumed to be 3μm centered at the origin. In this case, the total volume variation of the mitochondria is about 11.6% as compared with the case of 400nm mitochondria distributed in the 5μm cell models. The nucleus size variation effect was studied assuming that the nucleus radius is changed to 3.15μm while centered at the origin, and there are 180 mitochondria with radius of 400nm and the overall cell size is 5μm. This corresponds to a nucleus volume variation of about 11.6% as compared with the case of a 3μm nucleus with overall cell size of 5μm. Besides these two cases, we also considered the effects of cellular shape variation on the two-parameter light scattering plots method. We assume a cell has an ellipsoidal shape with the three semi-axes of sizes 5.0μm, 4.9μm and 4.8μm. There are also 180 mitochondria of radius

#104397 - $15.00 USD Received 21 Nov 2008; revised 1 Jun 2009; accepted 15 Jul 2009; published 20 Jul 2009

400nm and a nucleus of radius 3μm centered at the origin. In such a case, the cell volume variation is about 5.9% as compared with the 5.0μm cell models with distributed mitochondria.

The results for these three realizations with randomly distributed mitochondria are shown in Fig. 2(d). The upper half open sign shows the result for the realization of a cell model with a random distribution of mitochondria with a radius of 420nm. The lower half open sign shows the result for a mitochondrial random distribution with a nucleus radius of 3.15μm. And the left half open sign shows the result for the ellipsoidal cell model. The integrated intensity in the small angle range of 0 to 5 degrees is 0.7132 (arb. u.), 0.713 (arb. u), and 0.7247 (arb. u) for these three realizations, respectively. Compared with the mean of 0.7234 (arb. u.) for the eight realizations of randomly distributed mitochondria, the mean for these three realizations and the eight realizations of randomly distributed mitochondria is 0.7236 (arb. u.). Thus random mitochondrial distributions can still be well differentiated from the cases of mitochondrial aggregation to the nucleus periphery or mitochondrial aggregation to the membrane as shown in Fig. 2(d). Having considered the variations of the different biological cell components, the two-parameter light scattering plots method developed here is a promising technique for differentiating mitochondrial distributions in biological cells.

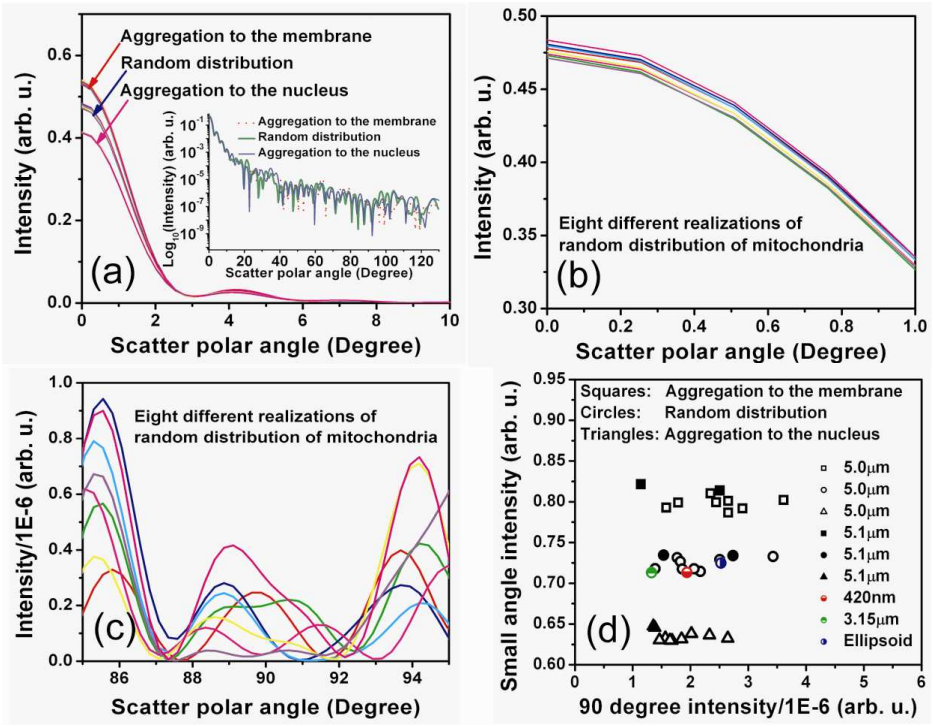

Fig. 2. A method for differentiating mitochondrial distributions in single biological cell models. (a), light scattering spectra from different cell models in the scatter angular range 0~10 degrees. (b), "zoomed in" results for the case of a random distribution of mitochondria as shown in (a). (c), eight realizations of random distribution of mitochondria in the scatter angular range 85~95 degrees. (d), two-parameter light scattering plots for differentiating different mitochondrial distributions.

In conventional cytometry, measurements of the small angle forward scatter intensity (0~5 degrees) are used to determine cell sizes [17,18]. The above results in this paper have shown that the mitochondrial distributions in a biological cell can change the small angle forward scatter intensity distributions. In this case, measurements of the small angle forward scatter intensity are not accurate for biological cell size determination. We have recently developed a Fourier transform method for size determination of micro-scale beads [19]. A Fourier

#104397 - $15.00 USD Received 21 Nov 2008; revised 1 Jun 2009; accepted 15 Jul 2009; published 20 Jul 2009

transform method for size determination of biological cells with complex inner structures is now introduced.

Figure 3(a) shows the light scattering spectra for four different cell models each with a cell radius of 5μm (three models for the different mitochondrial distributions generated with the same random seed and one model without mitochondria) over a wide angle side scatter range (57.5~122.5 degrees). This is the angular range that may be detected by the recently reported microfluidic cytometer [19] and the intensity fluctuations in this angular range can be well characterized by a Fourier analysis. Fourier transforms are performed on these light scattering spectra (Fig. 3(a)) and are shown in Fig. 3(b). The Fourier spectra show that there is a consistent typical frequency component for the four different cell models at frequency 0.3231 (1/Degree). Note here we refer to the location of the typical frequency component but not the frequency component amplitude. This highest dominant frequency determines the homogeneous spherical scatterer size [19], and corresponds here to the overall size of the biological cell models. Compared with the Fourier spectra from the cell model without mitochondria, the mitochondria inside biological cells contribute many larger amplitude frequency components lower than this typical peak frequency (Fig. 3(b)), especially in the frequency range 0.1 to 0.2 (1/Degree). Fourier transforms are also performed on the other twenty one realizations of mitochondrial distributions in biological cell models (5μm in radius) as used in Fig. 2(a) in the angular range 57.5~122.5 degrees. The Fourier spectra of these realizations further confirm that the location of the typical peak at a frequency 0.3231 (1/Degree) for the 5μm biological cells with distributed mitochondria.

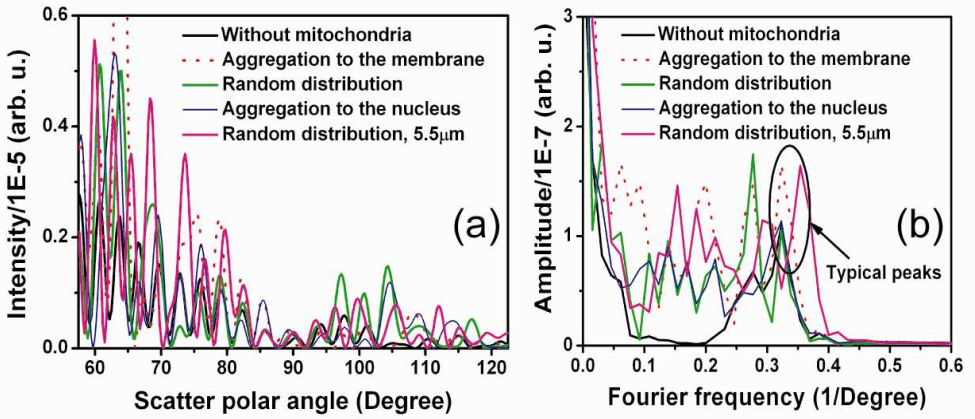

Fig. 3. A Fourier transform method for better determination of biological cell sizes. (a), light scattering spectra from different cell models in the angular range 57.5~122.5 degrees. (b), Fourier transforms of the light scattering spectra as shown in (a).

In order to determine whether the above discussed Fourier analysis method can be used for differentiating the size of biological cells with distributed mitochondria, a biological cell with radius of 5.5μm is considered. This realization also has 180 mitochondria (400nm in radius), and a nucleus of 3μm in radius centered at the origin. The Fourier analysis of the wide angle side scatter in the angular range 57.5 to 122.5 degrees of this realization (Fig. 3(a)) has a typical peak at frequency 0.3539 (1/Degree) (Fig. 3(b)). Compared with the 5μm cell models which have a typical peak at 0.3231 (1/Degree), the frequency variation is about 0.0308 (1/Degree) for the size variation of 500nm. Since the Fourier analysis we used here has a resolution of 0.0154 (1/Degree) in frequency, the Fourier analysis performed here can have a resolution of 250nm when estimating the size of a biological cell. This resolution may be further improved by performing a Fourier analysis on a wider light scattering angular range with a shorter wavelength illumination [19]. Considering both the cases for biological cell models with different mitochondrial distributions and biological cell overall size changes with distributed mitochondria, the Fourier analysis method shown here may be used for estimating the size of a biological cell even with distributed mitochondria within the cells.

#104397 - $15.00 USD Received 21 Nov 2008; revised 1 Jun 2009; accepted 15 Jul 2009; published 20 Jul 2009

4. Conclusions

In summary, different idealized cell models with distributed mitochondria generated via Monte Carlo simulations were developed. In the case of a "normal cell" model, the mitochondria were assumed to aggregate to the nuclear periphery, while in the case of a "cancer cell" model, a random mitochondrial distribution was assumed. Three dimensional FDTD simulations were performed on these different cell models. Analyses of the FDTD light scattering spectra showed that small angle forward scattering in two-parameter light scattering plots can be used to differentiate the different mitochondrial distributions that exist in these two cases. To the best of our knowledge, this is the first time that a quantitative characterization of mitochondrial distributions in single biological cells has been performed via light scattering simulations. In a recent paper by Wang et al. [20], the small angle forward scattering was measured in a microchip flow cytometer. In our previous publications, we reported the measurements of wide angle side scattering in an integrated microfluidic waveguide cytometer [19]. The integration of a Lab-on-a-chip (LOC) apparatus may be used to measure both the small angle forward scattering and wide angle side scattering in a flow cytometer. This suggests that the light scattering method for the differentiation of mitochondrial distributions in single biological cell models shown here has the potential of differentiating normal cells from cancerous ones.

The mitochondria inside the biological cell models change the small angle forward scatter intensity distributions as in the FDTD simulations. In this case, measurements of the small angle forward scatter intensity to determine cell sizes may not always be an accurate method. Here we have shown that the location of the highest dominant frequency component, not the frequency component amplitude, in the Fourier spectra of the wide angle light scattering may be used to determine size of single biological cells containing distributed mitochondria. The use of a Fourier analysis to separate the mitochondrial distribution and the cell volume effects on the small angle forward scatter intensity is worthy of future development. That is, the highest dominant frequency component could be used to infer the biological cell size, and the other frequency components may potentially be used to infer the mitochondrial distributions. This however requires new parameters to be found in the Fourier analysis of the 1D scatter spectra or alternatively from a 2D Fourier analysis of the 2D scatter patterns.

Acknowledgements

The authors thank WestGrid (University of Alberta, Canada) for the parallel computation support. This work is supported by the Natural Sciences and Engineering Research Council (NSERC) of Canada.

#104397 - $15.00 USD Received 21 Nov 2008; revised 1 Jun 2009; accepted 15 Jul 2009; published 20 Jul 2009